12

Monte Carlo Simulation of Insulating Gas Avalanche Development

Dengming Xiao
Dept. of E.E., Shanghai Jiaotong University, 200030
China

1. Introduction

SF_6 gas has excellent physical and chemical properties: general, chemical stability, not easy to react with other substances; not flammable and explosive, high security and reliability; in particular, to have a very high dielectric strength and destroy arc performance, so the existing power system in gas-insulated equipment, most of them are using pure SF_6 gas as insulating medium. The one of the most serious problem of SF_6 as insulating gas is that the "Kyoto Protocol" on the proposed global warming potential (GWP) in 1997. Its GWP is 23,900 times of CO_2, at the meeting clearly to reduce the gas as the future or even prohibit the use of the high-pollution gas. Reducing the environmental impact of greenhouse gases has become a research hotspot in recent years.

c-C_4F_8 is a colorless, odorless, nonflammable gas; and its GWP for the 8700, is one-third of SF_6, the impact on the environment is far less than the SF_6; and the gas completely is non-toxic, non-ozone impact. c-C_4F_8 in the low energy range has a high attachment cross section of in the uniform electric field. The dielectric strength of c-C_4F_8 is about 1.3 times to the SF_6 gas. c-C_4F_8 gas used for insulation is existing the shortcomings of expensive, discharge decomposition of conductive particles, and relatively higher liquefaction temperature. By adding N_2, CO_2 and other buffer gases of inexpensive, lower liquefied temperature and without the existence of carbon decomposition to c-C_4F_8 gas, c-C_4F_8 gas discharge characteristics can be improved. Buffer gas through the scattering of the electron energy can reduced electronegative gas to attached the energy range, hindering the avalanche growth, and the dielectric strength of c-C_4F_8 gas mixtures is reduced less than pure c-C_4F_8 gas.

c-C_4F_8 gas mixtures as a dielectric applications has attracted the attention of international experts on electricity and environmental. In 1997 the U.S. Institute of Standards and Technology considered the c-C_4F_8 gas mixture as a potential future long-term studies insulated gas; 2001 Tokyo Electric Power Industry Center research institutions and the University of Tokyo proposed the application of c-C_4F_8 gas mixtures as the insulating medium. This article will use the Monte Carlo Simulation (MCS) to study the gas mixtures discharge characteristics of c-C_4F_8 and N_2, CO_2 and CF_4 mixed composition.

In the gas discharge, we can not predict the trajectory of one electron, but there are a lot of electron, statistical methods can be used to analyze the randomness of the large number of electron. Avalanche development is effected mostly by the electrical force. From a macro point of view, the electron trajectory is a curve in electric field. Speaking from the micro electronic movement in the gas itself has a random nature. An electron leaved from

emission source, which point in the direction of motion collision was accidental, but has some probability distribution; and gas molecules in multiple collision scattering, the elastic collision in non-electronegative gas, or collisional excitation and impact ionization, may occur. In terms of the electronegative gas, may also occur attached, and there are a variety of collision probability; the energy and direction after the collision has to comply with a certain probability distribution. In electronegative gas, electron may be absorbed by molecular, then the electron movement came to an end, otherwise, continue to the next movement. An electron movement of gas in electric field can be reflected through the collision. Here, necessary to point out that the decision of the location in next collision and the determined direction and energy after the collision are only concerned with this collision, with nothing to do with electron collision before. To suppose that the density of gas molecules is not denseness, there is no chemical reaction between molecules under the conditions, which c-C_4F_8 gas, and N_2, CO_2 and CF_4 gas molecules is satisfied this condition. Random collision occurred in only under the conditions, the Monte Carlo model of establishment and improvement used to calculate the avalanche development of the mixed-gas in this paper.

2.1 Monte Carlo simulation model of gas avalanche flow chart

In this paper, uniform electric field E in the flat model is introduced. The electron in motion collide with gas molecules, including ionization collisions, excitation collision, elastic collision, which particles produced after the excited state collide also with other electrons and molecules. These processes are random, and the Monte Carlo method can be used to describe these processes. In the space of electronic sample, a certain number (eg 10000) of the simulation electrons sampled, then these electrons state of motion at a given moment statistics is followed and recorded. All electrons are sampled after the electrons moved some time, used to calculate. Figure 2.1 shows the Monte Carlo simulation model of gas discharge avalanche flow chart, followed by the detailed simulation of avalanche development process. Simulation process as follows:

1. sampling a certain number of simulation electrons,
2. calculating the flight time of an electron ,
3. calculating the movement time of the electron in flight time and the change of the location and speed of the electron,
4. deciding the collision type of the electron in flight time,
5. determining the electron state and the direction of movement after occuring the collision of electron,
6. finishing the movement of the electron in given time,
7. repeating the above process for each electron,
8. sampling the velocity, displacement and the number of all electrons in the same sampling interval, to calculate the discharge parameters of the drift velocity, the effective ionization coefficient and so on.

2.2 Monte Carlo simulation model of gas avalanche

2.2.1 Initialization of simulation electrons

While t = 0, a large number of electrons of isotropic distribution are released from the emission source, which are the average energy of 1ev (this energy is small enough to not affect the behavior of avalanche). The electrons gain energy under the electric field, and lose energy while it collides with gas molecules. Suppose the density of the gas molecules $3.32 \times 10^{16} cm^{-3}$ (i.e. the pressure is 1Torr, temperature is 20 ^{o}C), The electron density is small enough to ignore Coulomb effects between electrons.

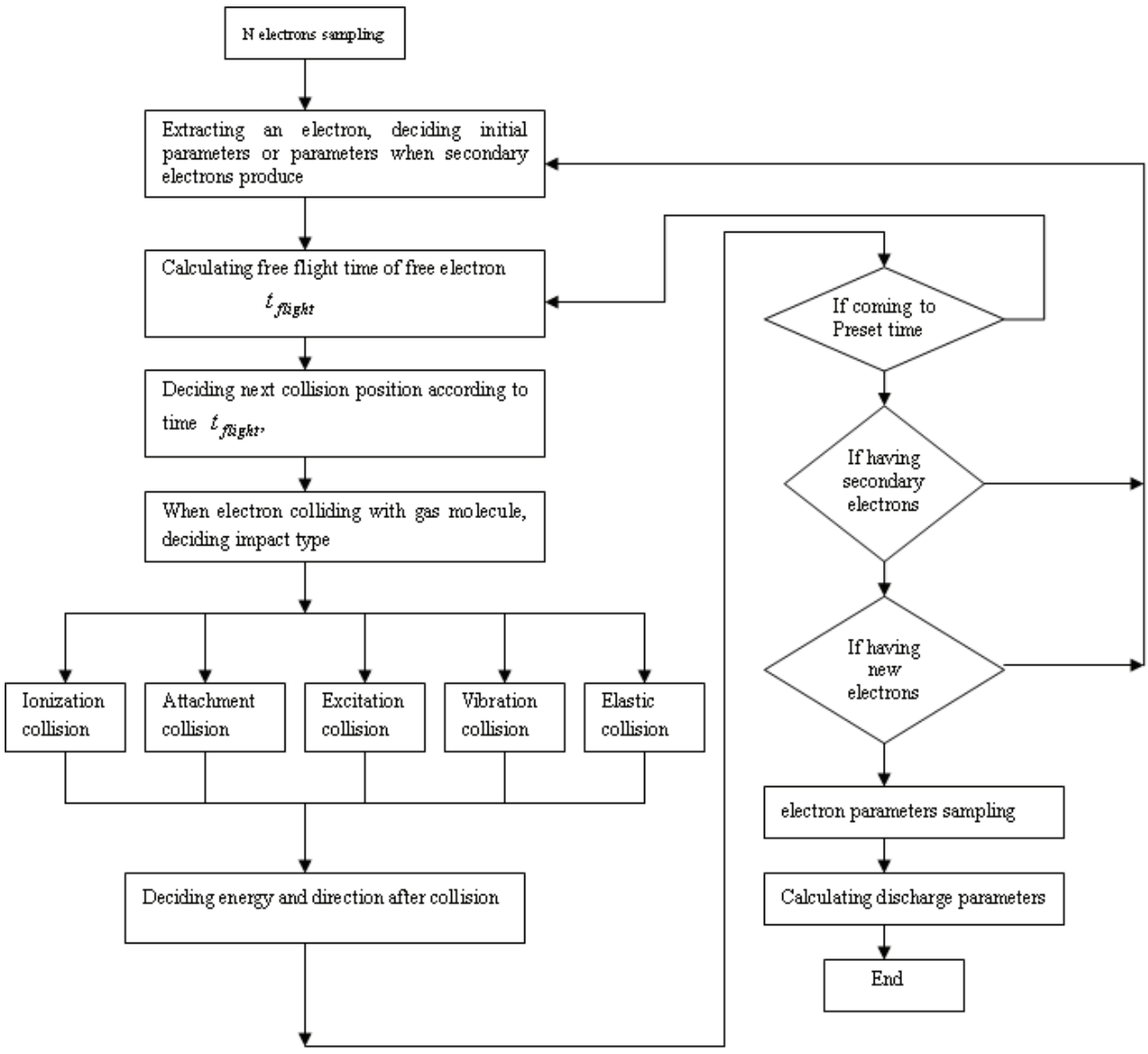

Fig. 2.1 Monte Carlo simulation model of gas discharge avalanche flow chart

2.2.2 Determination of electronic flight time

Electronic flight time is calculated in two ways, first using a simple approximation method, using the mean free flight time or the average collision distance, which spent time of a mean free path, another method being randomized to decide.

1. The average collision distance model

In the uniform electric field, the electron moves along the parabola trajectory until a collision with gas molecules. The average collision distance λ is:

$$\lambda = \frac{1}{N\sigma_{total}(\varepsilon)} \tag{2.1}$$

Which $\sigma_{total}(\varepsilon)$ is the total collision cross section, in units of cm², N is the density of gas molecules number, electronic energy ε. $\sigma_{total}(\varepsilon)$ is a function of energy, obviously λ depends on the electron energy. The mean free path is divided into small segments

$\Delta s = \lambda / k$. In a step distance, the probability of collision of the electron and gas molecules is:

$$P = 1 - \exp(-N\sigma_{total}(\varepsilon)\Delta s) \tag{2.2}$$

Collision occurs or not is determined by a random number ξ , that is, when P is less than the above calculated, the collision occurred. If no collision, then simulation electrons continue to next step in the movement; if a collision occurs, the number of electron and electron energy changes are determined according to the class of the crash. The whole process will be repeated in the next step until the electron is attached or reach to the set termination conditions.

2. The average collision time model

The average collision time of move with drift rate $W(\varepsilon)$:

$$T_m = \frac{1}{N\sigma_{total}(\varepsilon)W(\varepsilon)} \tag{2.3}$$

$W(\varepsilon)$ is the electron drift velocity.

Used to simulate the average collision time, because a calculation of electron energy changes is so larger that potential error occurs, the actual calculation of the average flight time will be divided into shorter time periods to calculate. Each step is calculated as:

$$dt = \frac{T_m(\varepsilon)}{K} \tag{2.4}$$

For large enough K, the collision frequency can be considered in the dt to be constant, then the collision probability in dt is:

$$P = 1 - \exp(-\frac{dt}{T_m}) \tag{2.5}$$

Using the mean free path or average time of flight, the status of each point in the sequence represents no longer one collision process. A free path or free flight time is divided into a lot of calculation steps, although the accuracy improved, but also causing the increase of computation. For c-C_4F_8, SF_6 and other electronegative gas, in order to improve the stability of the simulation, will track more the initial electron. Therefore, previous researchers introduced the concept of free flight time to improve the average flight time method, to enhance the computing speed.

3. free flight time

Probability of electron collision in the free flight time t_{flight} is:

$$p = f_{total} \cdot t_{flight} \tag{2.6}$$

In the formula f_{total} is the total collision frequency, which is a function of time. Set Q (t) is the probability of no collision of electron from 0 to t times, then the probability of no collision from 0 to t + t_{flight} time is:

$$Q(t + dt) = Q(t)(1 - P) = Q(t)(1 - f_{total} \cdot t_{flight}) \tag{2.7}$$

Taking the limit, so $t_{fligh} \to 0$, find:

$$\frac{dQ}{dt} = -f_{total}(t) \cdot Q(t) \tag{2.8}$$

$$Q(t) = \exp[-\int_0^{t_c} f_{total}(t)dt] \tag{2.9}$$

The formula is the probability Q (t) expression of no collision of the electron from 0 to t_c moment, thus the probability of collision in t_c is 1-Q (t_c). To determine when the collision of the electron occurs is to sample in the division. Producing a [0,1] uniform random number ξ in the formula and the following represents a uniform distribution random number between 0 and 1:

$$1 - Q(t_c) = \xi \tag{2.10}$$

In principle, the collision time $t = t_c$ can be obtained from the above two formulas, but then a more complex and time-consuming, because the total collision frequency with time-related will be integrated in the above two formulas. If the total collision frequency is constant, the problem is much better. At this point, it can be set outside the integral sign, then formula (2.10) becomes:

$$t_c = -\frac{In(1-\xi)}{f_{total}} \tag{2.11}$$

As for the ξ is [0,1] random number, then $1-\xi$ is [0,1] interval, the formula is changed to:

$$t_c = -\frac{In(\xi)}{f_{total}} \tag{2.12}$$

In fact, the total collision frequency is always time-related, because the formula for calculating the collision frequency :

$$f_{total} = n_{t\arg et}\sigma(\varepsilon) \cdot \upsilon_{relative} \tag{2.13}$$

It is the function of the electron energy (or speed). Electron move in electric field, and its speed will be changed, and not uniform motion. In order to simplify the calculation of flight time, the null collision method is a good way.

4. null collision

Previous calculation of free flight time, we have seen, if the total electron collision frequency and energy is independent, the calculation of the free flight time will be very simple. In fact electron is accelerated by the field, and its energy is changing, and therefore the total collision frequency will be relation with electron energy, and it will change as the electron energy, the calculation of free flight time can not use the above formula , and will be involved in integration. To deal with this problem is to introduce the concept of null collision, i.e. known as virtual self scattering process by some literatures, and it is a fictitious collision. This process is characterized by its collision frequency so choose - to make the process of the collision and the other collision have the sum of a constant collision frequency. Thus, the total collision frequency is constant, and energy independent. Thus,

when calculating electron collision, it will be very convenient, no matter how the change in electron energy free flight time can be calculated with a formula. Otherwise, having no null-collision case, the electron energy increased significantly in a free flight, then the total collision cross section is to change, the problem of calculation time of the free movement will occur. But without using the above formula, the calculation of free time would complicate. After using the concept of this method is very clear, but when occuring a collision, the collision is not necessarily true, there probably is a real collision, and the collision may be null (no collision). If the collision occurs null, the electron state in motion will remain unchanged, and speed and direction of motion does not change too.
To find the true maximum of the total collision frequency, $f_{\max} = \max[f_{total}(\varepsilon)]$, so the free time of flight can be obtained:

$$t_c = -\frac{In(\xi)}{f_{total}} \tag{2.14}$$

From the above description, the null collision method only requires the total collision frequency to be constant, how to choose it does not affect the calculation of free flight time. However, the selection of null collision frequency directly affect the simulation complexity and speed, and there are many kinds of null impact process on the selection. This article has improved the method, and the traditional and improved methods are described specifically in Section 2.3.

2.2.3 determination of the collision point position, the speed and energy

To set the electron affect only by electric fields, the electron in free flight time satisfy the energy conservation law, as the electron affect only by the electric field in the z-axis force, so in i +1 time the speed of the collision points are:

$$v_x^{i+1} = v_x^{i'} \tag{2.15}$$

$$v_y^{i+1} = v_y^{i'} \tag{2.16}$$

$$v_z^{i+1} = v_z^{i'} + \frac{eq}{m} t_{flight} \tag{2.17}$$

Position and energy of electric field are:

$$x^{i+1} = x^i + v_x^i \cdot t_{flight} \tag{2.18}$$

$$y^{i+1} = y^i + v_y^i \cdot t_{flight} \tag{2.19}$$

$$z^{i+1} = z^i + v_z^i \cdot t_{flight} + \frac{1}{2}\frac{eq}{m} t_{flight}^2 \tag{2.20}$$

2.2.4 Determination of the collision type

In gas discharge, the moving electrons collide with ions and atoms, and the collision type of each process is according to the collision frequency in proportion to the total collision

frequency distribution, which is a random process. The determination of the scattering direction after the collision and speed after scattering is also a random process.

To determine the collision type, the collision of the electron and which kind of gas molecules should be first determined. The collision is the assumption that the density of gas molecules is not big, and there is no chemical reaction between molecules, which occurs only under the conditions of random collisions. According to the statistical physics point of view, the collision probability of the electron and each molecule can first determine, then the collision probability of the electron and various molecules is determine. In this paper, the c-C_4F_8 and N_2, CO_2 and CF_4 gas molecules in the chemical stability is to satisfy this condition.

Setting the gas make up of the A, B, C three kinds of molecules, the molecular density units (number of molecules in cubic centimeters) are N_A, N_B, N_C, then the total frequency of electron collision in gas is:

$$f_t^m(\varepsilon_i) = f_t^A(\varepsilon_i) + f_t^B(\varepsilon_i) + f_t^C(\varepsilon_i) \tag{2.21}$$

Which $f_t^A, f_t^B, f_t^C, f_t^m$ are respectively the total collision frequency of A, B, C and the mixture gas. They are defined as follows:

$$f_t^A = N_A \sigma_t^A(\varepsilon_i) v \tag{2.22}$$

$$f_t^B = N_B \sigma_t^B(\varepsilon_i) v \tag{2.23}$$

$$f_t^C = N_C \sigma_t^C(\varepsilon_i) v \tag{2.24}$$

As the electron collision frequency is the collision possibility of of electron and molecules, so the probability of collisions of it with A, B, C molecules is respectively:

$$P_A = f_t^A / f_t^m \tag{2.25}$$

$$P_B = f_t^B / f_t^m \tag{2.26}$$

$$P_C = f_t^C / f_t^m \tag{2.27}$$

Easy to determine the collision of electron with which type molecules using standard sampling methods, this article only consider the case of two gas mixtures, then:

$$f_t^m(\varepsilon_i) = f_t^A(\varepsilon_i) + f_t^B(\varepsilon_i) \tag{2.28}$$

Among:

$$f_t^A = N_A \sigma_t^A(\varepsilon_i) v \tag{2.29}$$

$$f_t^B = N_B \sigma_t^B(\varepsilon_i) v \tag{2.30}$$

then the collision probability of two gases are:

$$P_A = f_t^A / f_t^m \tag{2.31}$$

$$P_B = f_t^B / f_t^m \tag{2.32}$$

Determining the collision of electron with which kind of molecular, then the collision type is determined according to the following method.

The collision of electron with gas molecules can occur on impact, such as elastic, scattering, excitation, ionization and attachment, etc.. The total collision frequency of electron and molecular is:

$$f_t = N\sigma_{el}v + N\sigma_{ex}v + N\sigma_i v + N\sigma_a v \tag{2.33}$$

Where f_t is the total collision frequency, $\sigma_{el}, \sigma_{ex}, \sigma_i$ and σ_a are respectively the elastic collision cross section, excitation cross sections, ionization cross sections and attachment cross sections.

For the excitation cross section can be further broken down:

$$N\sigma_{ex}v = N\sigma_{ex1}v + N\sigma_{ex2}v + N\sigma_{ex3}v + \cdots \tag{2.34}$$

General:

$$N\sigma v = \sum_j N\sigma_j v \quad \sigma = \sum_j \sigma_j \tag{2.35}$$

Where j is collision types, $\sigma_{ex1}, \sigma_{ex2}, \sigma_{ex3}, \cdots$ are the the collision cross section of different excited levels respectively.

The microscopic cross section of the gas mixtures are represented by $\sigma_{el}^A, \sigma_{ex}^A, \sigma_i^A$ and σ_a^A (this article used A to represent c-C_4F_8 in dealing with mixture) and $\sigma_{el}^B, \sigma_{ex}^B$, and σ_i^B (B on behalf of non-electronegative gas such as N_2,CO_2), said that

$$\sigma_t^A = \sigma_{el}^A + \sigma_{ex}^A + \sigma_i^A + \sigma_a^A \tag{2.36}$$

$$\sigma_t^B = \sigma_{el}^B + \sigma_{ex}^B + \sigma_i^b \tag{2.37}$$

The occuring probability of various collision can be determined as follows.

If the electron and mixed gas molecule A (c-C_4F_8) collided, then the occuring probability of various collision are:

$$P_{el}^A = \frac{\sigma_{el}^A}{\sigma_{el}^A + \sigma_{ex}^A + \sigma_i^A + \sigma_a^A} \tag{2.38}$$

$$P_{ex}^A = \frac{\sigma_{ex}^A}{\sigma_{el}^A + \sigma_{ex}^A + \sigma_i^A + \sigma_a^A} \tag{2.39}$$

$$P_i^A = \frac{\sigma_i^A}{\sigma_{el}^A + \sigma_{ex}^A + \sigma_i^A + \sigma_a^A} \tag{2.40}$$

$$P_a^A = \frac{\sigma_a^A}{\sigma_{el}^A + \sigma_{ex}^A + \sigma_i^A + \sigma_a^A} \tag{2.41}$$

If the electron and mixed gas molecule B (other non-electronegative gas molecules) collided, then the occuring probability of various collision are:

$$P_{el}^{B} = \frac{\sigma_{el}^{B}}{\sigma_{el}^{B} + \sigma_{ex}^{B} + \sigma_{i}^{B}} \tag{2.42}$$

$$P_{ex}^{B} = \frac{\sigma_{ex}^{B}}{\sigma_{el}^{B} + \sigma_{ex}^{B} + \sigma_{i}^{B}} \tag{2.43}$$

$$P_{i}^{B} = \frac{\sigma_{i}^{B}}{\sigma_{el}^{B} + \sigma_{ex}^{B} + \sigma_{i}^{B}} \tag{2.44}$$

using standard sampling methods, the collision type can be easily determined.

2.2.5 Determination of electron state after the collision

After occurring the electron collision, the electron will change the direction of movement (if it will attache to disappear, no longer considered), and the energy is also changing. For different processes, the change is not the same. The energy of elastic collision of electrons does not change almost, but the direction is changed; while ionization occurs, the energy and direction of the electron will be changed, but also creating a new electron; occurring excitation, electron energy and direction of motion will be changed.The random method is used to determine energy, speed and direction after occurring the collision.

1. Determination of the electron scattering angle and azimuth

As the electron energy and direction after collision is related, the electron scattering angle and azimuth are first determined. Scattering angle (or deflexion angle) is the angle of the scattering direction and the direction of the origina motion, and azimuth is angle around the axis of rotation. Typically, the probability density distribution of the azimuth φ is according to [0,2π] uniform distribution, as long as the [0,1] uniform random number ξ is drawn out, easy to calculate:

$$\varphi = 2\pi\xi \tag{2.45}$$

For the scattering angle χ , the produce of random numbers is sampled by the following formula :

$$\frac{2\pi}{\sigma_k(v)} \int_0^{\varphi} \sigma(v,\chi')\sin\chi' d\chi' = \xi \tag{2.46}$$

Seen from this formula, the scattering angle χ is the function of the electron velocity and the random number. Sampling method need to have differential collision cross section, assuming isotropic scattering, which $\sigma(v,\chi)$ does not rely on χ , $\sigma_k = 4\pi\sigma$ is gained from this formula, then differential collision cross section is $\frac{\sigma_k}{4\pi}$, and the probability of scattering in all directions are the same. At this point, the probability density of the deflection angle χ

is $\frac{1}{2}\sin(\chi)$, $\chi \in [0,\pi]$, and accordingly the isotropic distribution of the scattering angle cosine can be derived:

$$F(x) = 0.5 \quad x < [-1,1] \tag{2.47}$$

It can be directly sampled, resulting in [0,1] random number ξ , then

$$\cos(\chi) = 2\xi - 1 \tag{2.48}$$

$$\sin(\chi) = \sqrt{1-\cos^2(\chi)} \tag{2.49}$$

2. Determination of the direction cosine after scattering

Determined the direction angle before and after the collision ,namely the direction of the scattering angle χ and azimuth φ, the direction cosine (u_{m+1}, v_{m+1}, w_{m+1}) after the collision can be determined as follows:

$$u_{m+1} = \frac{(-bcw_m u_m - bdv_m)}{\sqrt{1-w_m^2}} + au_m \tag{2.50}$$

$$v_{m+1} = \frac{(-bcw_m v_m + bdu_m)}{\sqrt{1-w_m^2}} + av_m \tag{2.51}$$

$$w_{m+1} = bc\sqrt{1-w_m^2} + aw_m \tag{2.52}$$

Among

$$a = \cos\chi\,,\ b = \sin\chi = \sqrt{1-a^2} \tag{2.53}$$

$$c = \cos\varphi\,,\ d = \sin\varphi \tag{2.54}$$

while $1 - w_m^2 \to 0$, the formula can not be applied, to applied a simple formula:

$$u_{m+1} = bc \quad v_{m+1} = bd \quad w_{m+1} = aw_m \tag{2.55}$$

3. Determination of the electron energy and velocity after the collision

If the collision of electron with gas molecules is elastic, the electron energy after collision is:

$$\varepsilon_1 = \varepsilon_0[1 - \frac{2m}{M}(1-\cos\chi)] \tag{2.56}$$

Gas molecules are far more weight than electron, so the direction of electron is only changed and the energy of electron does not change basically.

If the excitation process of the electron with gas molecules occurs, then

$$\varepsilon_1 = \varepsilon_0 - \varepsilon_j \tag{2.57}$$

In the formula, ε_1 is the energy after scattering and the energy ε_0 for before scattering. ε_j is for the energy loss in the excitation process, usually being the excitation energy. The remaining energy will be maintained by the electron.
If the ionization process of the electron with neutral particles occurs, the scattered electron energy and new energy produced secondary electron are distributed by the original remaining electron energy :

$$\varepsilon_{reminder} = \varepsilon_1 - \varepsilon_{ion} \tag{2.58}$$

$$\varepsilon_1^{'} + \varepsilon_2^{'} = \varepsilon_{remainder} \tag{2.59}$$

In the formula, neglected the energy of neutral gas molecules and new ion, $\varepsilon_1^{'}$ is the electron energy after scattering, and $\varepsilon_2^{'}$ is the electron energy produced from the ionization, and ε_{ion} is the electron energy loss in ionization process. How the two electron energy are allocated? This is correlateion with electron energy differential ionization cross sections $\sigma(\varepsilon, \varepsilon_c)$, which can be determined generated a random number ξ by the following formula, namely to determine the incidence electron collision energy.

$$\xi = \frac{\int_0^{\varepsilon_1^{'}} \sigma(\varepsilon_0, \varepsilon) d\varepsilon}{\sigma_i(\varepsilon_0)} \tag{2.60}$$

In the formula, ε_0 is the energy before the electron collision, and $\varepsilon_1^{'}$ is the potential energy of main electron after the collision, and $\sigma_i(\varepsilon_0)$ is the total ionization cross sections. As the gas ionization energy differential cross sections do not find ready-made data, so the method of random allocation is only introduced. Produced uniform random number ξ between [0,1], then

$$\varepsilon_1^{'} = \varepsilon_{remaider}\xi \tag{2.61}$$

$$\varepsilon_2^{'} = \varepsilon_{remaider}(1-\xi) \tag{2.62}$$

The size of electron speed can be calculated with energy:

$$v = \sqrt{\frac{2\varepsilon}{m}} \tag{2.63}$$

The velocity component in x, y and z axis can be calculated according to the direction cosine:

$$v_x = vu_{m+1} \quad v_y = vv_{m+1} \quad v_z = vw_{m+1} \tag{2.64}$$

To continue calculating the electron move in the next free flight time, it will be calculated to the set time. After tracking a large number of electron movement, then sampling and calculating electron data, the gas discharge parameters can be got.

2.2.6 The sampling and calculation of record data

After the simulation process, the sample processing in the records results is need. The methods of sampling and calculation are different corresponding to different experimental

methods. Here are three kinds of experimental methods involved in sampling and calculation methods.

1. SST(Steady State Townsend) experiment

To simulate SST, experimental results must generate a large number of consecutive initial electron, and to form a stable electron flow need to track enough long time, so calculation is exceedingly large amount, then sampling method is:

$$\overline{\omega}(x) = \frac{\sum_{j=1}^{N} \omega_j \Delta t_j}{\sum_{j=1}^{N} \Delta t_j} \tag{2.65}$$

Here, ω_j is the sampling data of the j electron in x to $x + \Delta x$, and Δt_j is the time of the electron through the region x to $x + \Delta x$, and N is the total number of electron in the region, and $\overline{\omega}(x)$ is the sample data in the location. The method is rarely used because of spending many time.

2. TOF(Time Of Flight) experiment

For the TOF experiment, the sampling and calculation are carried out according to the following.

ionization coefficient

$$a = In(1 + n_{ion} / N_{i-1}) / (z_i - z_{i-1}) \tag{2.66}$$

attachment

$$\eta = In(1 + n_{att} / N_{i-1}) / (z_i - z_{i-1}) \tag{2.67}$$

the drift velocity in avalanche center is defined as

$$W_r = \frac{d\overline{z}}{dt} \tag{2.68}$$

here

$$\overline{z}(t) = \int_{-\infty}^{+\infty} z p(z,t) dz \tag{2.69}$$

$$p(z,t) = \frac{n(z,t)}{\int_{-\infty}^{+\infty} n(z,t) dz} \tag{2.70}$$

here n (z, t) is the electron density distribution at t time, then W_r is defined as:

$$W_r = \frac{(1/N_2)\sum_{j=1}^{N_2} x_j(t_2) - (1/N_1)\sum_{j=1}^{N_1} x_j(t_1)}{t_2 - t_1} \tag{2.71}$$

Axial diffuse coefficient is defined as

$$D_L = \frac{1}{2}\frac{\partial}{\partial t}\int_{-\infty}^{+\infty} [z - \overline{z}(t)]^2 p(z,t) dz \tag{2.72}$$

Therefore

$$D_L = \frac{1}{2}\frac{[\frac{1}{N_2}]\sum_{j=1}^{N_2}[z_j(t_2)-\overline{z}_j(t_2)]^2 - [\frac{1}{N_1}]\sum_{j=1}^{N_1}[z_j(t_1)-\overline{z}_j(t_1)]^2}{t_2-t_1} \tag{2.73}$$

3. PT(Pulsed Townsend) experiment

For the PT experiment, the electronic properties and its position in the avalanche is correlation, therefore the sampling method conducted by the following

$$\overline{\omega}(t) = \frac{\int_{-\infty}^{+\infty}\int_0^{\infty}\omega F(\varepsilon,x,t)d\varepsilon dx}{\int_{-\infty}^{+\infty}\int_0^{\infty}F(\varepsilon,x,t)d\varepsilon dx} = \frac{\sum_{j=1}^{N_t}\omega_j}{N_t} \tag{2.74}$$

ω_j is the value of J electron at t time in avalanche, and N_t is the total number of electron at t time in avalanche, then the avalanche parameters is calculated as follows:

$$W_v = \frac{\overline{z}}{t} \tag{2.75}$$

$$a = \frac{In[(n/n_0)+1]}{\overline{z}} \tag{2.76}$$

The formula and the $n = n_0\exp(az-1)$ in the Townsend equation is the same, in the case of ionizing absence

$$\eta = \frac{n^-}{n^+}\frac{1}{\overline{z}} \tag{2.77}$$

In the case of ionization

$$\eta = \frac{n^-}{n^+}a \tag{2.78}$$

Horizontal and vertical diffusion coefficients have the following definitions

$$D_L(t) = \frac{1}{2t}\frac{d}{dt}\overline{(z_t-\overline{z}_t)^2} = \frac{1}{2t}\frac{d}{dt}\overline{(z_t{}^2-\overline{z}_t{}^2)} \tag{2.79}$$

$$D_r(t) = \frac{1}{2t}\frac{d}{dt}\overline{\{\frac{1}{2}(x^2+y^2)\}} \tag{2.80}$$

Therefore

$$D_L = \frac{\overline{z^2}-\overline{z}^2}{2t} \tag{2.81}$$

$$D_r = \frac{\overline{r^2}}{4t} = \frac{\overline{x^2+y^2}}{4t} \tag{2.82}$$

Here v_e is the drift velocity, a and η are ionization and attachment coefficients respectively, and $\bar{z}$ is the average distance of motion in a sample model time to the t time.

2.3 Improved Monte Carlo simulation model for the development of avalanche in gas

Contraposing the disadvantage of traditional null collision method, a new Monte Carlo simulation of avalanche development model has been proposed in this section.

While t = 0, a large number of electrons of the average energy of 1ev isotropic distribution are released from the emission source, the electrons gained energy under the electric field, and they will lose energy as colliding with gas molecules. Suppose the density of the gas molecules is $3.32\times10^{16}cm^{-3}$ (i.e. the pressure is 1Torr, temperature is 20 ^{o}C), The electron density is small enough to ignore the Coulomb interaction between electrons.

1960 S L Lin proposed the null collision Monte Carlo method, to improve its speed, which was cited later by a large number of reference literatures. However the null collision process use the difference of the total collision frequency and the maximum, which citing by the most of author, all cross sections considered must be processed in each step in the simulation process. The null collision method only requires the total collision frequency to be constant, how to choose does not affect the calculation of free flight time. However, the selection of null collision frequency directly affect the simulation complexity and speed, and many kinds of null collision process may be selected. This article is going to set the collision frequency limit for each collision process, then needing only to calculate a cross-section can complete the simulation of gas avalanche development at each interval, to enhance further the calculation speed.

2.3.1 The traditional Monte Carlo null collision method

The traditional way to select a null collision frequency, being cumulative frequency of each collision process, get the real total collision frequency, and find the maximum value $f_{\max}$ of null collision frequency, and it is the difference of the total collision frequency and the maximum. On this approach, the selected time has two ways: the process set method and pre-set method.

The process set method is to set $f_{\max}$ in the interval following the experience and according to the electron motion state in each time period, which value is different in different time periods. However, the simulation process should consider two cases, if a free flight time $f_{\max}$ is always the maximum value of the total collision frequency, then the collision occurred in the end time of free flight time, and the new maximum limit of collision frequency is set in next state, to continue the simulation process. However, as H.R.SKULLERUD pointed out, $f_{\max}$ is the difficult choice: In principle, $f_{\max}$ should be made as small as possible to improve computational efficiency in each interval ; but if $f_{\max}$ made too small, so that $f_{null}<0$ in a certain energy point and the time interval, then the procedure must return to the point of $f_{null}=0$, to re-select simulation, to makes the code very complex.

Pre-set method is to set the maximum of the total the collision frequency in the range of interest energy before the start of the simulation. As shown in Figure 2.2 (ν_i shown the corresponding real frequency in i-collision process), it pre-calculate the sum of the collision frequency in all energy range of interest, taking the maximum $f_{\max}$ of sum. This method has the advantage of eliminating the trouble of computing time than the set method, but having

the big null collision frequency, especially in the low energy range, wasting the calculation time of more null collision. The following describe in detail the traditional null collision Monte Carlo simulation process.

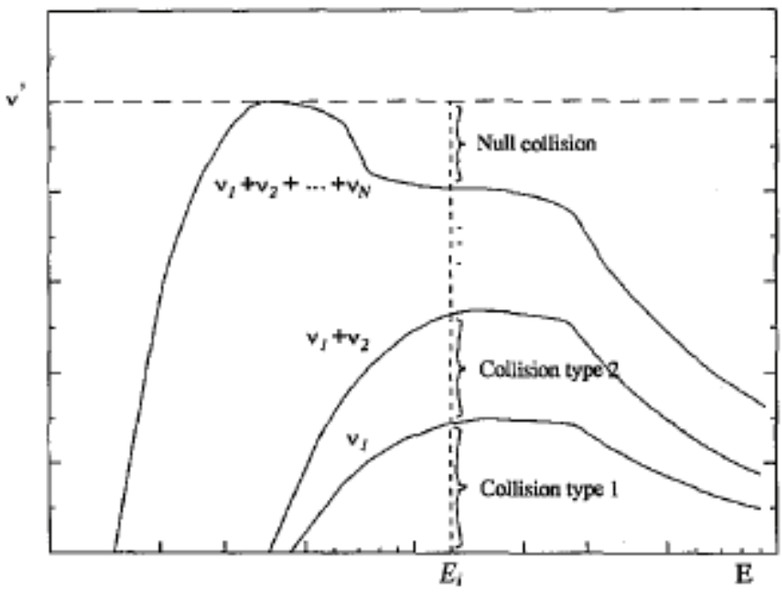

Fig. 2.2 Legend of traditional null collision Monte Carlo method

If describing the electron collision process with i=1….M, in one electron speed, most of the literature used in null collision with f_{null} :

$$f^i(v) = NQ^i(\varepsilon)v \tag{2.83}$$

$$f_{null} = f_{\max} - \sum_{i=1}^{M} f^i(v) \tag{2.84}$$

Where N is the density of gas molecules, $Q^i(\varepsilon)$ and $f^i(v)$ are the collision cross section and frequency corresponding to the i collision process. f_{null} is the null collision corresponding frequency to no cause any changes in gas properties. $f_{\max}$ is to make always f_{null} be positive constants, which is the effective collision frequency after introducing null collision . In order to continue the process of simulation, the actual flight time is:

$$t_{flight} = \frac{-1}{f_{\max}} In(\xi) \tag{2.85}$$

In the formula ξ and following ξ express the random number of a uniform distribution between 0 and 1.

Suppose the electron in moving process comply with the law of energy conservation, if to determine the free flight time, while tracking electronic collisions may occur the next time, the displacement and energy can be determined by the classical equation of energy

conservation. Before the next collision, the key is to determine the collision type and the gas molecules possible colliding with the electron.
Collision type will be decided by the random number between a uniform distribution in [0,1]:

$$\xi \le f_1(v_i) / f_{\max} \tag{2.86}$$

$$f_1(v_i) / f_{\max} < \xi \le (f_1(v_i) + f_2(v_i)) / f_{\max} \tag{2.87}$$

$$\sum_{j=1}^{N} f_j(v_i) / f_{\max} < \xi \tag{2.88}$$

If ξ meets the above equation, the corresponding collision type occurs. For example, when equation (2.88) set up, the null collision type occurs, then the electron does not occur any change.
From the above process can be seen, in order to determine the electron collision frequency and the collision type, all the gas collision cross section must be calculated in each time.

2.3.2 Improved null collision Monte Carlo method

In this paper, pre-setting an upper limit $f_{\max}^{i}$ for each collision process, the null collision frequency $f_{null}^{i}(\nu)$ corresponding to the i collision process can be obtained by upper limit $f_{\max}^{i}$ and the actual collision frequency $f^{i}(v)$:

$$f_{null}^{i}(v) = f_{\max}^{i} - f^{i}(v) \tag{2.89}$$

The collision frequency unit is sec^{-1}, taking into account the density of gas molecules, the ceiling of the total collision frequency will be:

$$f_{\max}^{tot} = \sum_{i}^{M} f_{\max}^{i} \tag{2.90}$$

The actual flight time will be:

$$t_{flight} = \frac{-1}{f_{\max}^{tot}} In(\xi) \tag{2.91}$$

First define

$$\xi_i = \frac{1}{f_{\max}^{tot}} \sum_{j=1}^{i} f_{\max}^{j} \tag{2.92}$$

if

$$\xi_{i-1} \le \xi < \xi_i \tag{2.93}$$

Set up, then the i collision process may occur, the same random number is used to determine whether such a collision is real, if

$$\xi - \xi_{i-1} < \frac{f^{(i)}(v)}{f_{\max}^{tot}} \tag{2.94}$$

Then the collision does occur.
From the above simulation, we can see that the collision type in each collision speed can be determined, only need to calculate a collision cross section.
In the article, the cross-section used are isotropic in the simulation process. in order to reduce the scattering angle, it can be assumed to be isotropic in the laboratory coordinates, to be uniformly distributed in [-1,1] range, so simulation format

$$\cos\theta = 2\xi - 1 \tag{2.95}$$

As the radius of the z-axis is symmetry, azimuth is:

$$\psi = 2\pi\xi \tag{2.96}$$

The energy and direction are determined according to collision type and isotropic angle after the collision.
Simulation in a continuous period of time is until a pre-set time. The energy and location of all electron (including the emergence of new electronic ionization) are sampled at a fixed time interval, then avalanche discharge parameters can be calculated by:
Electron drift velocity V_d :

$$V_d = \frac{d\overline{z}}{dt} \tag{2.97}$$

Effective ionization coefficient

$$\overline{a} = \frac{\overline{f}}{V_d} = \frac{1}{V_d}\frac{dIn(n/n_0)}{dt} \tag{2.98}$$

Where $\overline{z}$ and $\overline{f}$ are the average distance and the effective ionization frequency in the actual sampling moment of time t. n_0 and n are the number of electrons while time 0 and t. As $\overline{\alpha}/N = 0$, the gas dielectric strength $(E/N)_{\lim}$ can be educed.

2.4 The selection of gas collision cross section

Previous Monte Carlo simulation, the cross section area obtained by the experiments are needed all to carry on repeatedly modifying until the cross section area obtained by simulation and the gas discharge test parameters by measurement are consistent. With the development of computer technology, many researchers have adopted neural networks, genetic algorithms and numerical optimization methods to obtain the most data of gas cross section area, to provide a great convenience for future researchers. This article cited the cross section area in the literature to calculate.
In the Monte Carlo calculation, the method to obtain the desirable data are two forms of points cross section and often sub-section cross. In the sub-section, the energy scope of the problem is divided into many intervals, then the section data and energy are independent in each interval, and that is that the section data introduce the sub-section form. Point section refers to tracking particles, starting to find the required data of the each particles by energy

cross section library, then using interpolated method (or otherwise) find the appropriate section of the energy of the various data points, and the approximate formula can be constructed according to variation of characteristics of measured data, then this method is more direct and precise. In this paper, the point section method has been introduced according to known cross-section data.

2.4.1 c-C_4F_8 gas cross section

The measured data of c-C_4F_8 cross section are many, but more one-sided until 2001 Christophorou and JK Olthoff summarized the cross section of ionization, attachment and neutral decomposition. In 2004, by adjusting the vibration and momentum transformation section according to their basis, Masahiro Yamaji and Yoshiharu Nakamura et al summarized a set c-C_4F_8 cross-sectional area which Monte Carlo simulation data and measured discharge parameters of drift velocity, vertical diffusion coefficient, effective ionization coefficient are consistent. Their research has given a very accurate c-C_4F_8 gas cross-sectional area, especially in the low energy range, the cross section shown in Figure 2.3.

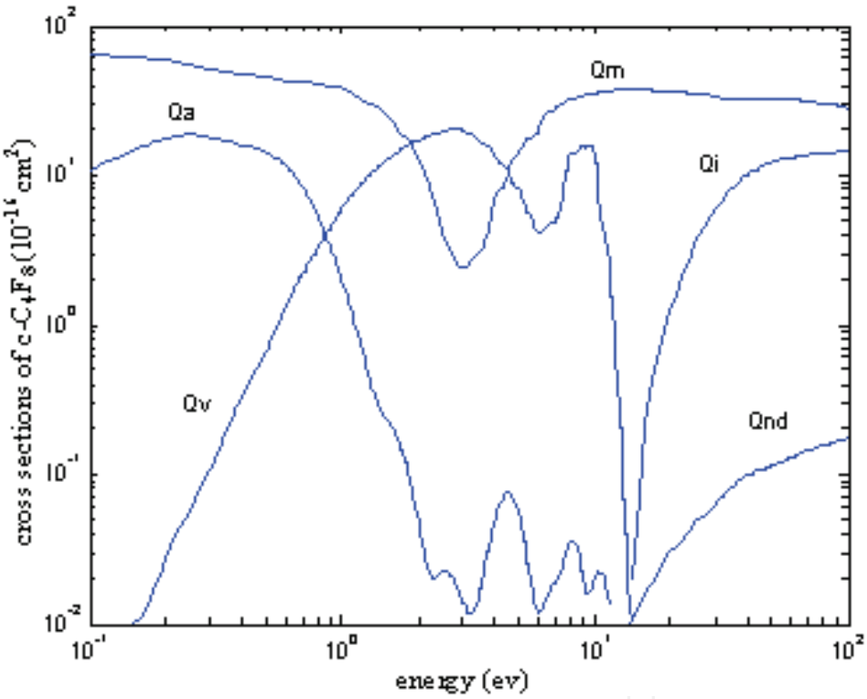

Fig. 2.3 Cross sections of c-C_4F_8 gas: (Qa), attachment; (Qv), vibration excitation; (Qnd), neutral dissociation; (Qi), ionization; (Qm), momentum transfer.

2.4.2 CF_4 gas cross section

This article cited the research data of Kurihara and others in literature, which summarized a set CF_4 cross section area, including 16 kinds of collisions: one elastic momentum transformation, three vibrational excitation and one electronic excitation cross section, one attachment section and seven neutral ionization cross sections and three neutral decomposition section. Kurihara et al have adjusted the decomposed cross-section, making the data and CF_4 gas discharge parameters of the experimental measurement be consistent.

Complete cross-section of the gas as shown in Figure 2.4, due to the corresponding section of the gas are more, Table 2.1 shows the collision process of the gas corresponding to the process ID and the threshold energy.

			Reaction	**Threshold (ev)**
(1)	Q_m	Momentum transformation	$CF_4 + e \rightarrow CF_4 + e$	
(2)	Q_{v1}	Vibration excitation	$CF_4 + e \rightarrow CF_4(v1) + e$	0.108
(3)	Q_{v3}	Vibration excitation	$CF_4 + e \rightarrow CF_4(v3) + e$	0.168
(4)	Q_{v4}	Vibration excitation	$CF_4 + e \rightarrow CF_4(v4) + e$	0.077
(5)	Q_{ex}	Electronic excitation	$CF_4 + e \rightarrow CF_4^{\,j} + e$	7.54
(6)	Q_a	Electronic Attachment	$CF_4 + e \rightarrow F^- + CF_3$	6.4
(7)	Q_{i1}	Neutral ionization 1	$CF_4 + e \rightarrow CF_3^+ + F + 2e$	16
(8)	Q_{i2}	Neutral ionization 2	$CF_4 + e \rightarrow CF_2^+ + 2F + 2e$	21
(9)	Q_{i3}	Neutral ionization 3	$CF_4 + e \rightarrow CF^+ + 3F + 2e$	26
(10)	Q_{i4}	Neutral ionization 4	$CF_4 + e \rightarrow C^+ + 4F + 2e$	34
(11)	Q_{i5}	Neutral ionization 5	$CF_4 + e \rightarrow F^+ + CF_3 + 2e$	34
(12)	Q_{i6}	Neutral ionization 6	$CF_4 + e \rightarrow CF_3^{2+} + F + 3e$	41
(13)	Q_{i7}	Neutral ionization 7	$CF_4 + e \rightarrow CF_2^{2+} + 2F + 3e$	42
(14)	Q_{d1}	Neutral decomposition 1	$CF_4 + e \rightarrow CF_3 + F + e$	12
(15)	Q_{d2}	Neutral decomposition 2	$CF_4 + e \rightarrow CF_2 + 2F + e$	17
(16)	Q_{d3}	Neutral decomposition 3	$CF_4 + e \rightarrow CF + 3F + e$	18

Table 2.1. CF_4 gas collisions process and the corresponding threshold energy

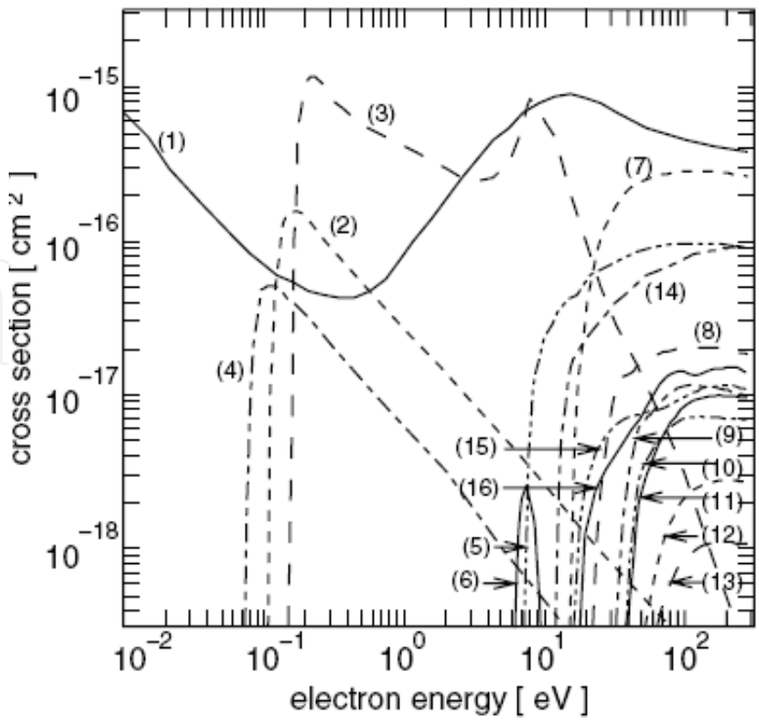

Fig. 2.4 CF_4 gas collision cross section

2.4.3 N_2 gas cross section

The N_2 cross section proposed by AV Phelps and LC Pitchford have been used, and Bolsigplus software package detailed description the section, including one momentum transfer, one rotation, nine vibration excitation, twelve electronic excitation, one single spectrum states, one ionization, considering twenty five of collision cross section. In the software literature describes in more detail.

2.4.4 CO_2 gas cross section

Kücükarpaci HN et al scientists have used Monte Carlo simulate the CO_2 gas avalanche motion in 1979, ordering a set of elastic and inelastic collision section.

2.4.5 SF_6 gas cross section

Since c-C_4F_8 gas mixtures need comparing with SF_6 gas mixtures, SF_6 gas cross section must be chosen. The cross-section sorted out by H. Itoh, Y and others have been used in this article, which including the momentum transformation, vibrational excitation, attachment, ionization and electronic excitation cross sections.

2.5 Experimental verification of the improved method

Now SF_6/N_2 gas mixtures have been applied in the power industry, however SF_6/ CO_2 gas mixtures may be superior to certain characteristics of SF_6/N_2 mixtures. For example, having the electrode conductive particles between the electrodes and the electrodes rough existing uneven electric field, SF_6- CO_2 has a higher insulation breakdown strength. SF_6 and CO_2 gas have therefore more reliable collision cross section and the gas discharge experiment data.

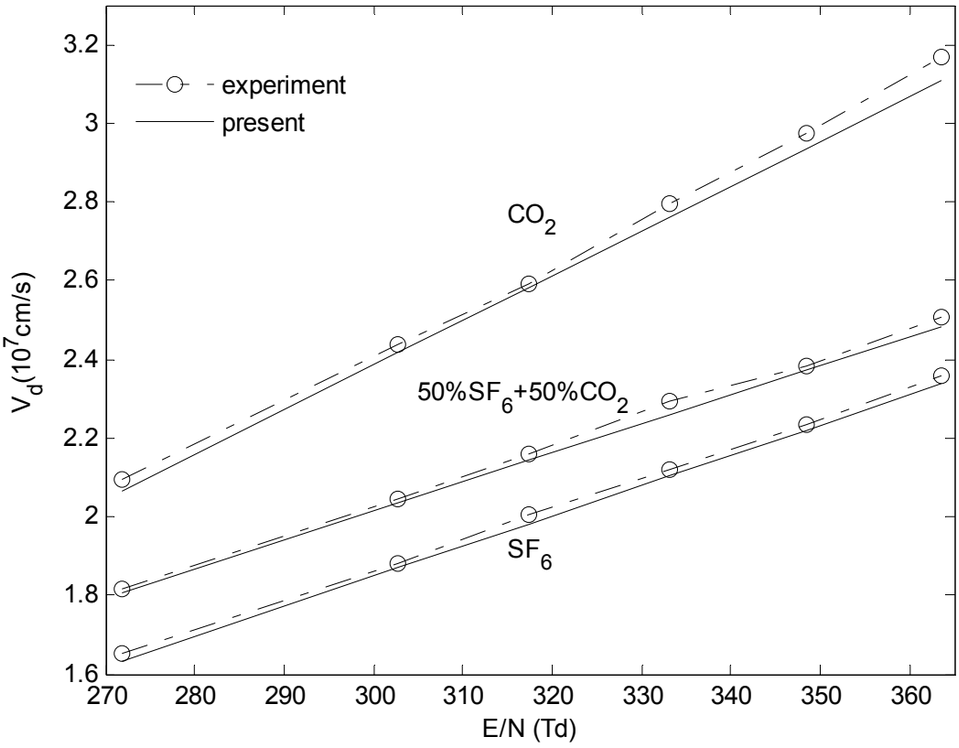

Fig. 2.5 Drift velocity of SF_6/CO_2 gas mixtures

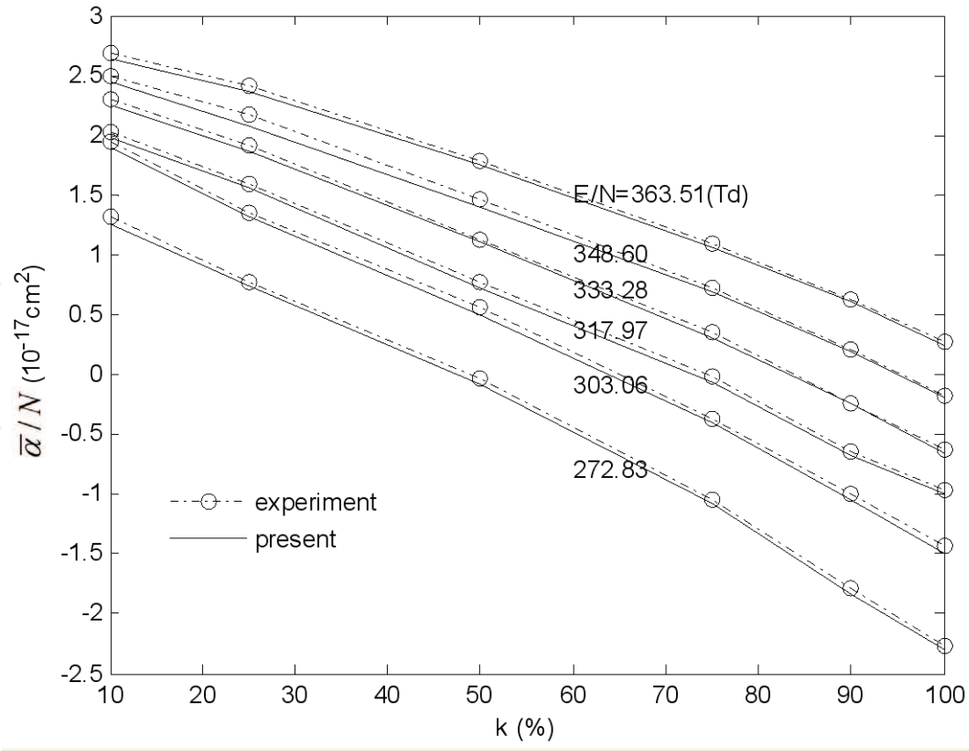

Fig. 2.6 $\overline{\alpha}/N$ of SF_6/CO_2 gas mixtures as a function of mixing ratio k at different E / N

In order to verify the Monte Carlo method to improve the accuracy, taking the reliable cross-sectional area of SF_6, CO_2, the improved Monte Carlo was used simulating the Pulsed Thomsond test process of SF_6- CO_2 gas mixtures, to find the drift velocity, effective ionization coefficient of the mixture, to calculate the critical breakdown field strength of the gas mixtures. The simulation results and experimental data were compared to verify the correctness of the modified method.

The electron drift velocity of SF_6, CO_2 and 50% SF_6 +50% CO_2 gas mixtures were shown in figure 2.5. Being seen from the graph, CO_2 is greater than SF_6 in the drift speed , and mixed-gas drift velocity is in between, to may be due to CO_2 gas adding to SF_6 gas, and the insulation strength of the gas mixtures is reduced. At different field strength E / N, the variation curves of the effective ionization coefficient $\overline{\alpha}/N$ as SF_6 concentration k was shown in figure 2.6, which decreased with the K value increases. In figure 2.5 and 2.6 the experimental data were also given to compare with the simulating data, which shows excellent consistency.

The variation of critical breakdown field strength $(E/N)_{lim}$ as k was shown in figure 2.7. The experimental values were also shown in the figure to contrast the simulating data, which showed good agreement, to show that use of the improved Monte Carlo method are feasible.

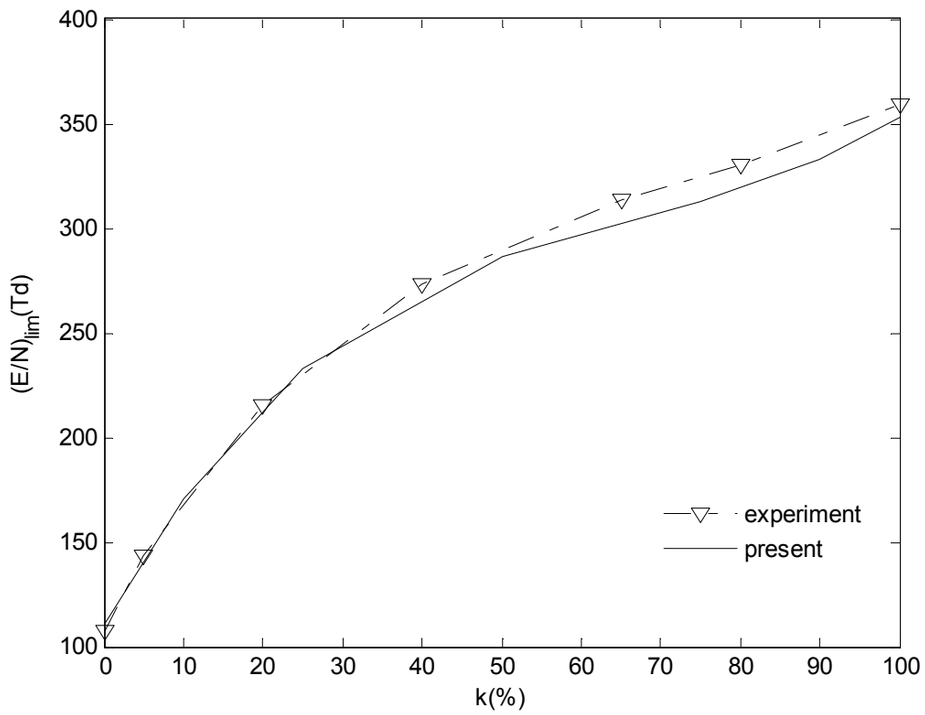

Fig. 2.7 Critical breakdown field strength of SF_6/CO_2 mixtures

2.6 Simulation of avalanche discharge in c-C_4F_8 gas mixtures

In this article, the cross section area of gas in reference and the improved Monte Carlo method have been used to simulate the avalanche development process of the c-C_4F_8 and N_2, CO_2, CF_4 gas mixtures, to calculate also the critical breakdown field, which were compared with the corresponding data of SF_6 gas mixtures in the figure. The measuring value of the

critical field strength in the previous literature was also given in the figure to compare with the simulation results to further validate the accuracy of the gas cross section and the improved Monte Carlo method.

Assuming at uniform electric field, the gas dielectric strength increased in proportion with the pressure, then gas pressure increased multiples of the mixture to reach the insulation strength of SF_6 gas was also calculated. At the same time the impact on the environment of the mixed gas used in insulating media, which rate of decline in the GWP, was also analysed.

2.6.1 The avalanche discharge parameters of c-C_4F_8 and N_2 gas mixtures

1. the effective ionization coefficient

The effective ionization coefficient as a function curves of field E/N at different mixture ratio in c-C_4F_8/N_2 gas mixtures were shown in Figure 2.8. Shown in the figure, $\overline{\alpha}/N$ decreased with the increase of c-C_4F_8 content, increased with the E/N value increases. This is because in the same field strength, c-C_4F_8 content was higher, then collisions probability of electron and c-C_4F_8 gas was higher, so the possibility of electron attachment increased to increase attachment coefficient, thus $\overline{\alpha}/N$ decreased; in the same c-C_4F_8 content, with the electric field strength increased, high-energy electrons increased, low energy electron decreased, thus $\overline{\alpha}/N$ increased.

2. electron drift velocity

Simulating drift velocity Ve of c-C_4F_8/N_2 gas mixtures was shown in Figure 2.9. With the c-C_4F_8 gas content k increased, at a fixed E/N value, the drift velocity Ve decreased significantly, which was beneficial from the insulation point of view. The Ve increased with E/N value increases at a fixed K value. The Ve of c-C_4F_8/N_2 gas mixtures was affected greatly by c-C_4F_8 gas.

3. the critical breakdown field strength

To order $\overline{\alpha}/N$ = 0, the critical breakdown field strength $(E/N)_{Lim}$ could be given at the different mixing ratio, which showed gas insulation strength due to uniform electric field. Shown from Figure 2.10, SF_6/N_2 gas mixtures at low mixing ratio, the critical breakdown field strength increased rapidly with SF_6 content k increase, but larger when mixing ratio, which tended to saturation; and the $(E/N)_{Lim}$ of c-C_4F_8/N_2 gas mixtures increased almost linearly with c-C_4F_8 content k increase. In the mixing ratio K is less than 60%, the insulation strength of c-C_4F_8/N_2 was lower than SF_6/N_2, but with the mixing ratio increases, the insulation strength of c-C_4F_8/N_2 was higher than the insulation strength of SF_6/N_2, which was 1.25 times of the latter in the mixing ratio of 100%.

4. the pressure required for the relative insulated intensity of SF_6

Figure 2.11 showed that c-C_4F_8/N_2 and SF_6/N_2 gas mixtures to reach the insulation strength of SF_6 gas required ratio of pressure and K. Shown from the figure, the two gas need to increase the pressure of gas mixtures to be similar multiples, when low mixing ratio the former was slightly higher than the latter. With increasing the content of c-C_4F_8, gas pressure needed to become smaller and smaller, at K= 40%, needed to increase 1.35 times, when the mixing ratio continues to increase, the required pressure of c-C_4F_8/N_2 and SF_6 was almost similar or even lower than SF_6.

5. c-C_4F_8/N_2 gas mixtures on the improvement of the environmental impact

Figure 2.12 showed the GWP ratio of the gas mixtures and pure SF_6 at the various mixing ratio, in which the greenhouse effect of c-C_4F_8/N_2 was far less than SF_6/N_2. In 40% of the

mixing ratio, the GWP of SF_6/N_2 was 40% of the SF_6, while the GWP of c-C_4F_8/N_2 was only 15% of SF_6, thus environmental impact was reduced.

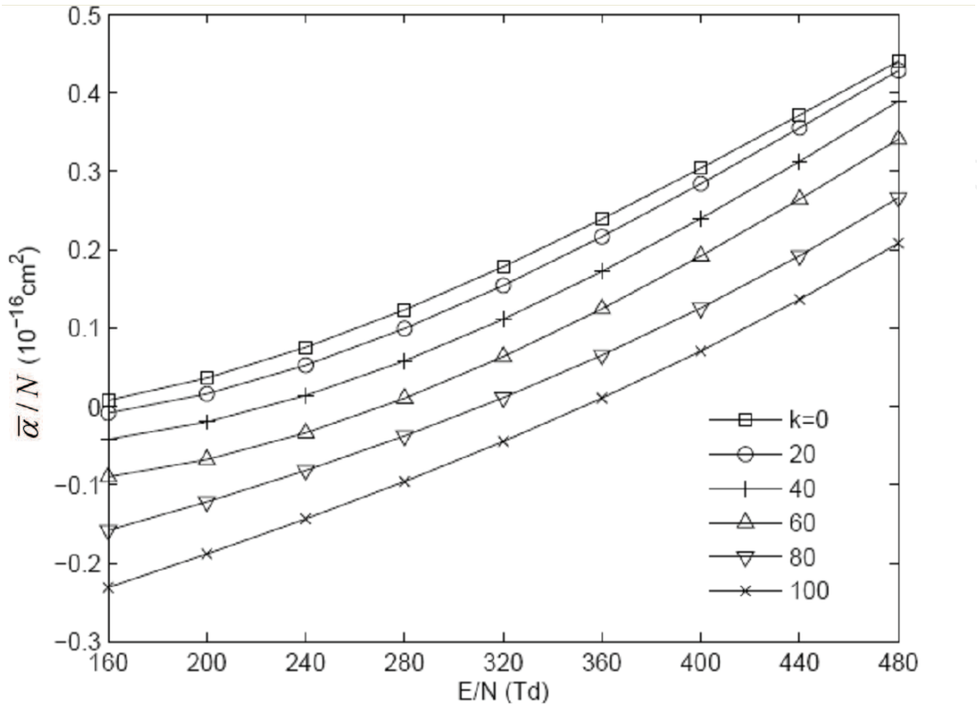

Fig. 2.8 $\overline{\alpha}/N$ of c-C_4F_8/N_2 gas mixtures as a function of E / N at different mixture ratio K

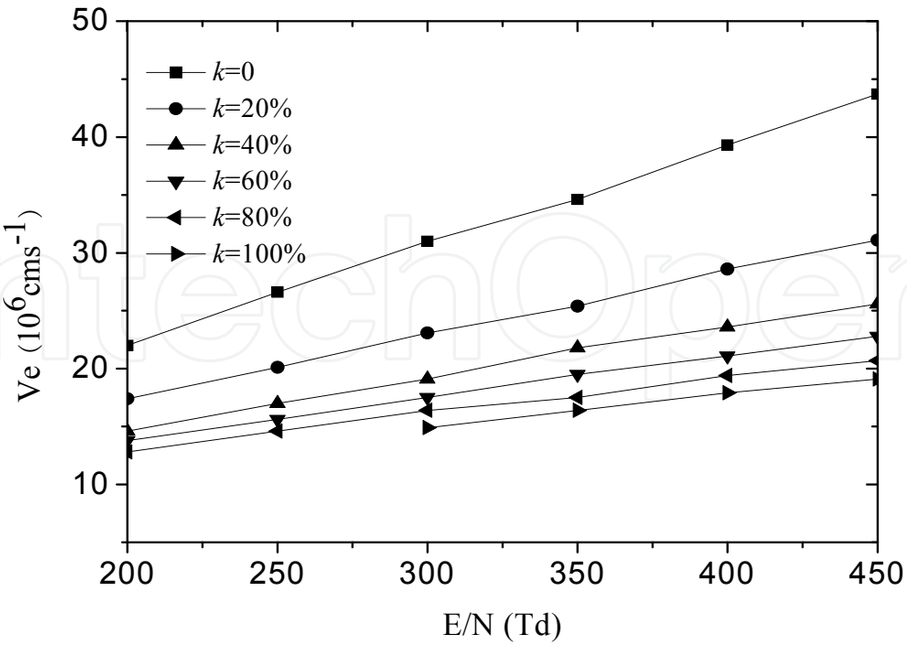

Fig. 2.9 The electron drift velocity Ve as function of E / N in c-C_4F_8/N_2 at different c-C_4F_8 content *k*

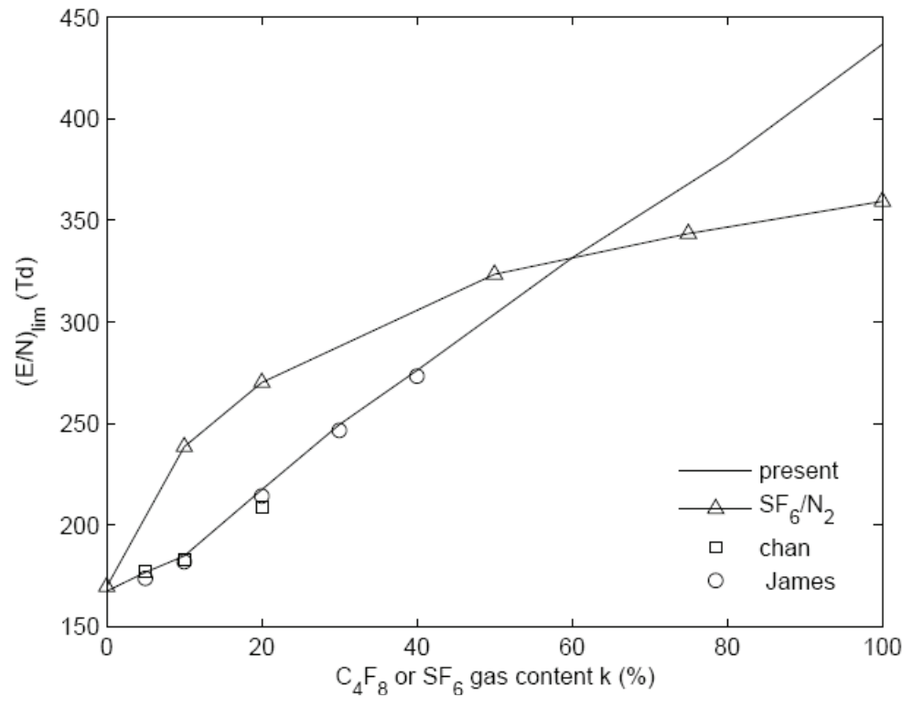

Fig. 2.10 $(E/N)_{Lim}$ of c-C_4F_8/N_2 gas mixtures as a function of c-C_4F_8 gas content k (experiment data: SF_6/N_2(Δ), c- C_4F_8/N_2 by James(○)and Chan (□))

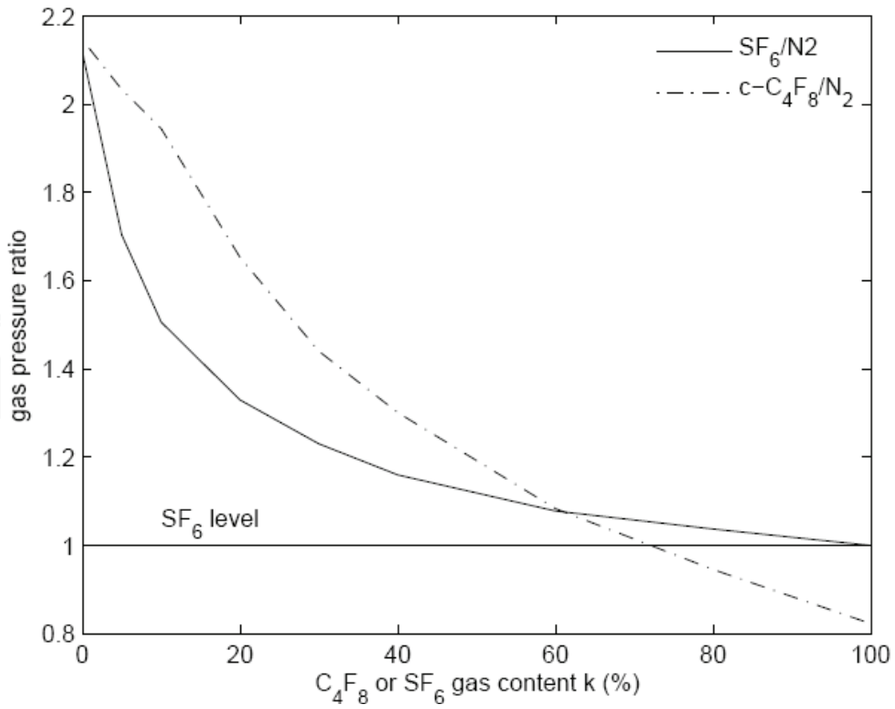

Fig. 2.11 Required gas pressure ratio of c-C_4F_8/N_2 gas mixtures comparable with insulation property of SF_6

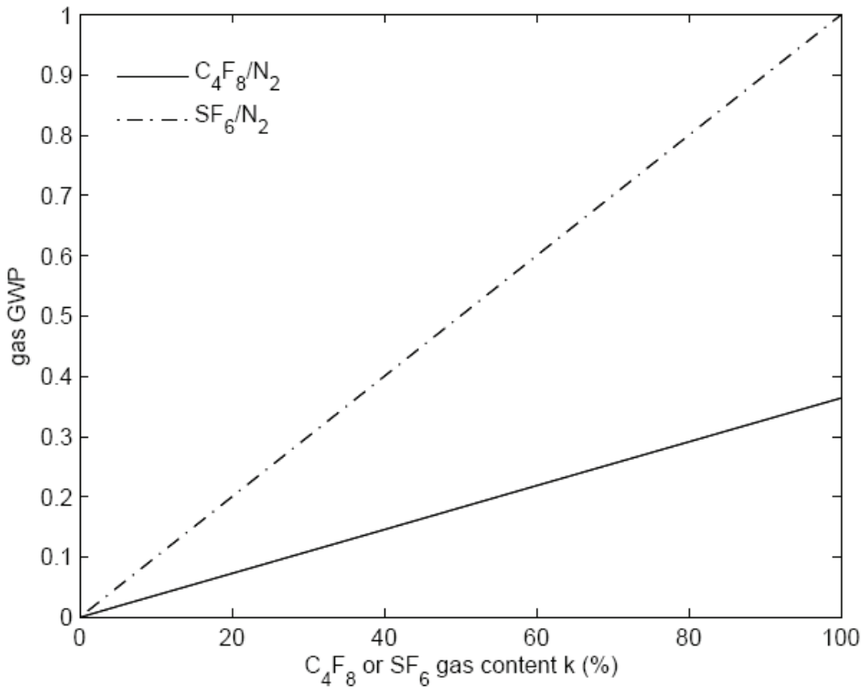

Fig. 2.12 GWP of c-C_4F_8/N_2 gas mixtures relative to pure SF_6

2.6.2 The avalanche discharge parameters of c-C_4F_8 and CO_2 gas mixtures

The effective ionization coefficient $\overline{\alpha}/N$ in c-C_4F_8/CO_2 gas mixtures as a function curve of the field strength E/N at different mixture ratio was shown in Figure 2.13, its variation was almost consistent with c-C_4F_8/N_2. $\overline{\alpha}/N$ decreased with the increase of c-C_4F_8 content, and it increased with E/N value increases.

The electron drift velocity V_e as function of E/N in c-C_4F_8/CO_2 mixtures at different c-C_4F_8 gas mixture ratios k was shown in Figure 2.14. With the c-C_4F_8 gas content k increases, at a fixed E / N value, the drift velocity Ve trend obvious downward. At K was same value, Ve increased with E / N value increases.

The critical breakdown field strength $(E/N)_{Lim}$ in c-C_4F_8/CO_2 gas mixtures as a function curve of c-C_4F_8 gas content k was shown in Figure 2.15. Shown from the figure, the curve variation was almost consistent comparing SF_6/CO_2. While the mixing ratio K was less than 60%, the $(E/N)_{Lim}$ of c-C_4F_8/CO_2 was less than the strength of SF_6/CO_2, but with the mixing ratio increases, the insulation strength of c-C_4F_8/CO_2 was greater than that of SF_6/CO_2 .

The ratio of needed pressure of c-C_4F_8/CO_2 and SF_6/CO_2 gas mixtures to reach the insulation strength of SF_6 was shown in Figure 2.16. With the c-C_4F_8 content increased, the gas pressure needed to become smaller and smaller, at K=40%, needed to 1.7 times, and when the mixing ratio continues to increase, the required pressure of c-C_4F_8/CO_2 was almost the same with SF_6 gas and SF_6/CO_2 gas mixtures.

The GWP ratio of c-C_4F_8/CO_2, SF_6/CO_2 gas mixtures and pure SF6 at the various mixing ratio was shown in Figure 2.17. The GWP of c-C_4F_8/CO_2 was far less tant of SF_6/CO_2. In 40% of the mixing ratio, the GWP of SF_6/CO_2 was 40% of GWP for the SF_6, but the GWP of c-C_4F_8/CO_2 was only 15% of GWP in SF_6, thus impact on the environment was much reduced.

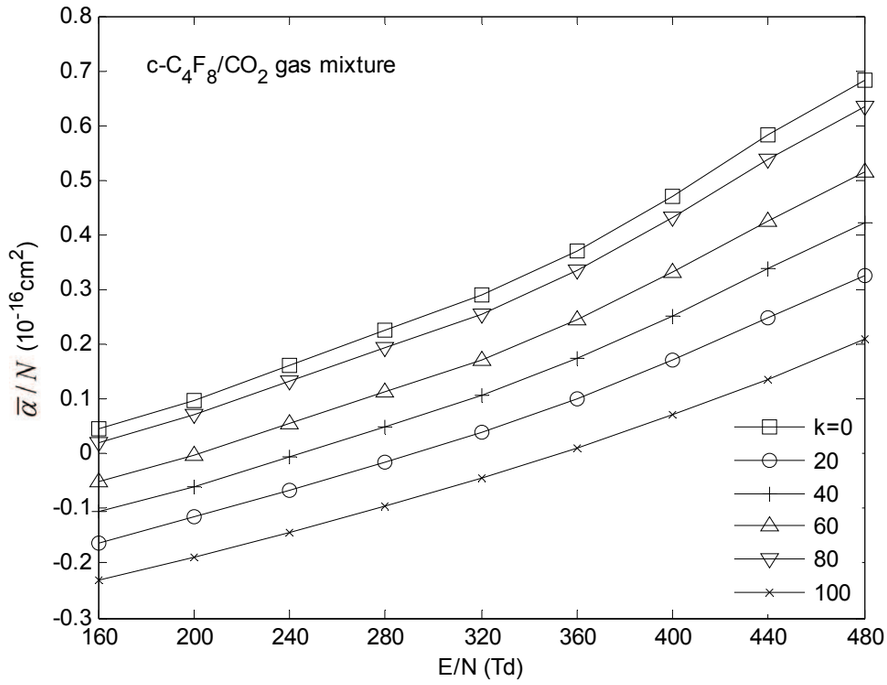

Fig. 2.13 $\overline{\alpha}/N$ in c-C_4F_8 and CO_2 gas mixtures as a function curve of E/N at different mixture ratio

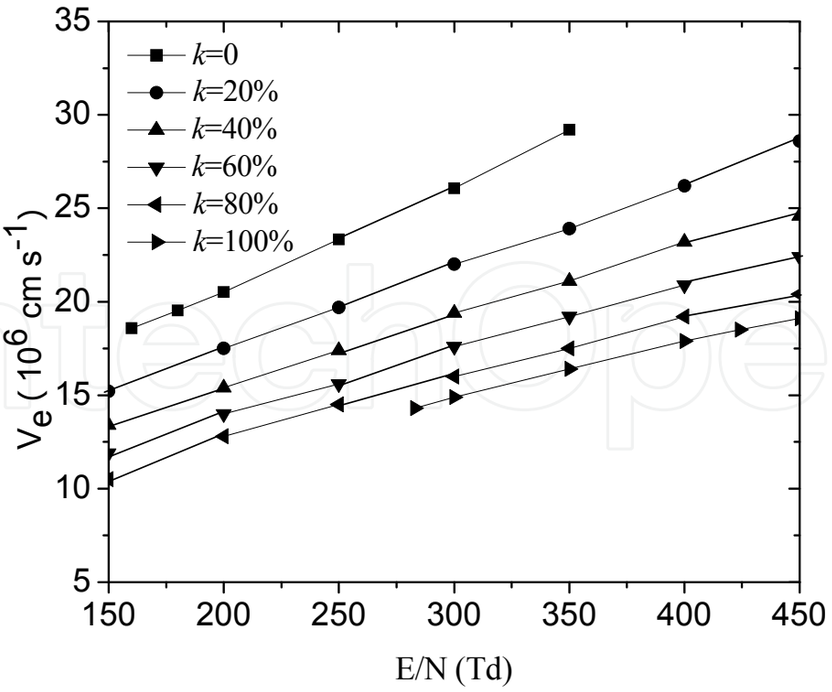

Fig. 2.14 The electron drift velocity Ve as function of E / N in c-C_4F_8/CO_2 mixtures at different c-C_4F_8 gas mixture ratios k

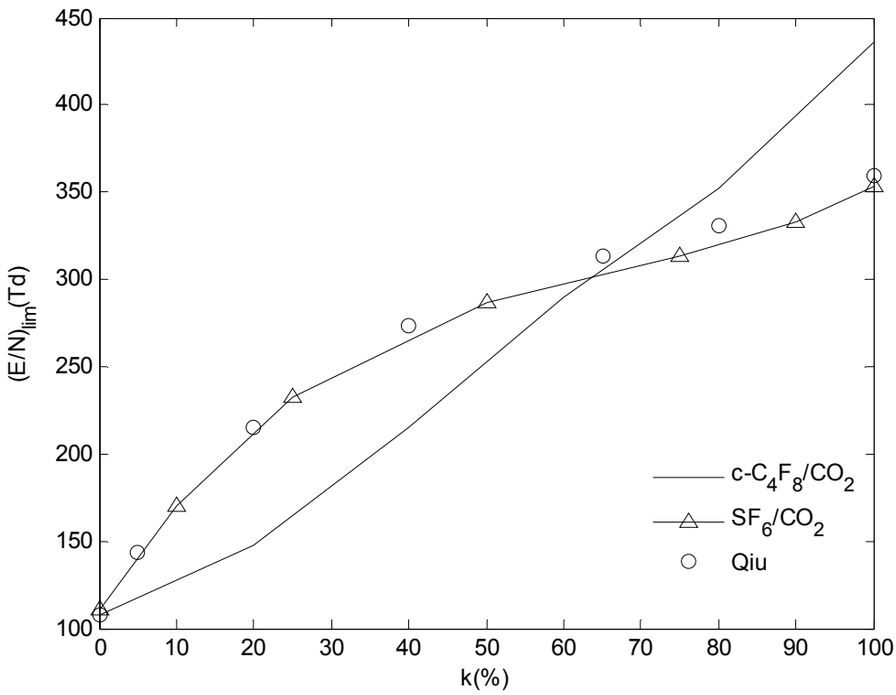

Fig. 2.15 $(E/N)_{Lim}$ of c-C_4F_8 and CO_2 gas mixtures as a function of c-C_4F_8 gas content k (experiment data: SF_6/CO_2 by Qiu)

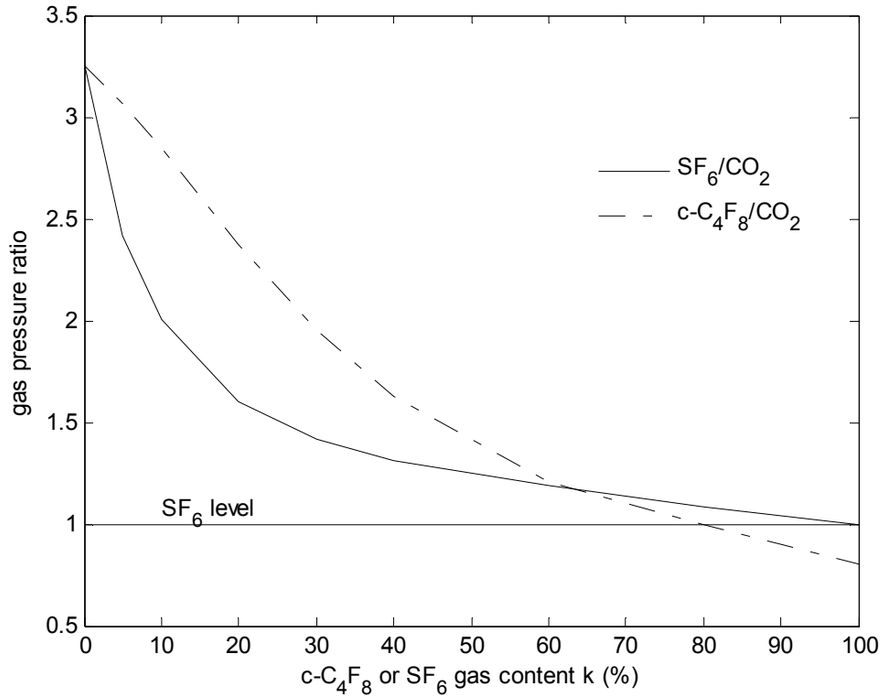

Fig. 2.16 Required gas pressure ratio in c-C_4F_8/CO_2 gas mixtures comparable with insulation property of SF_6

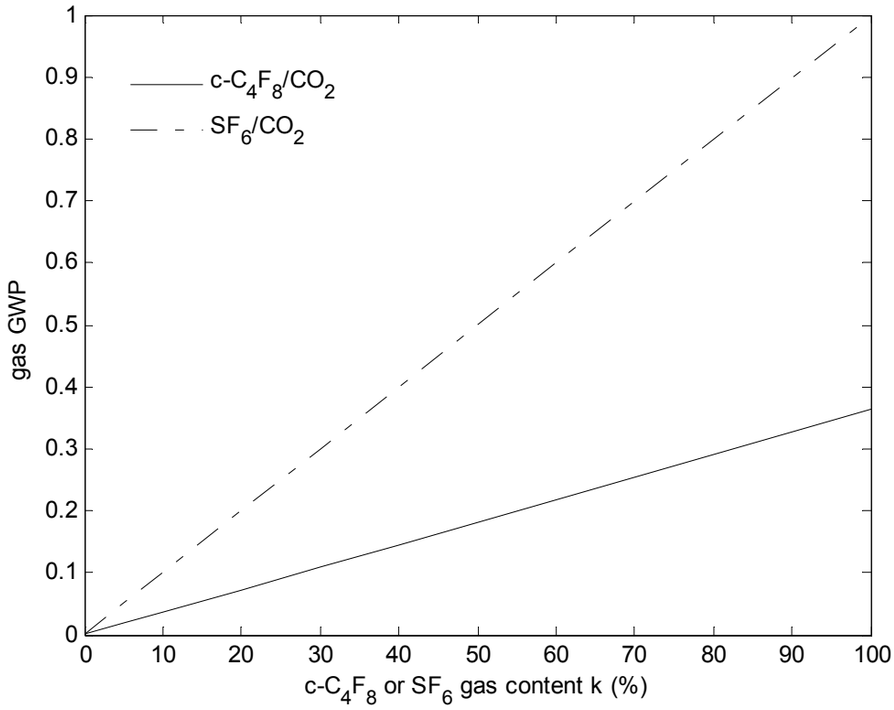

Fig. 2.17 GWP of c-C_4F_8 and CO_2 gas mixtures relative to pure SF_6

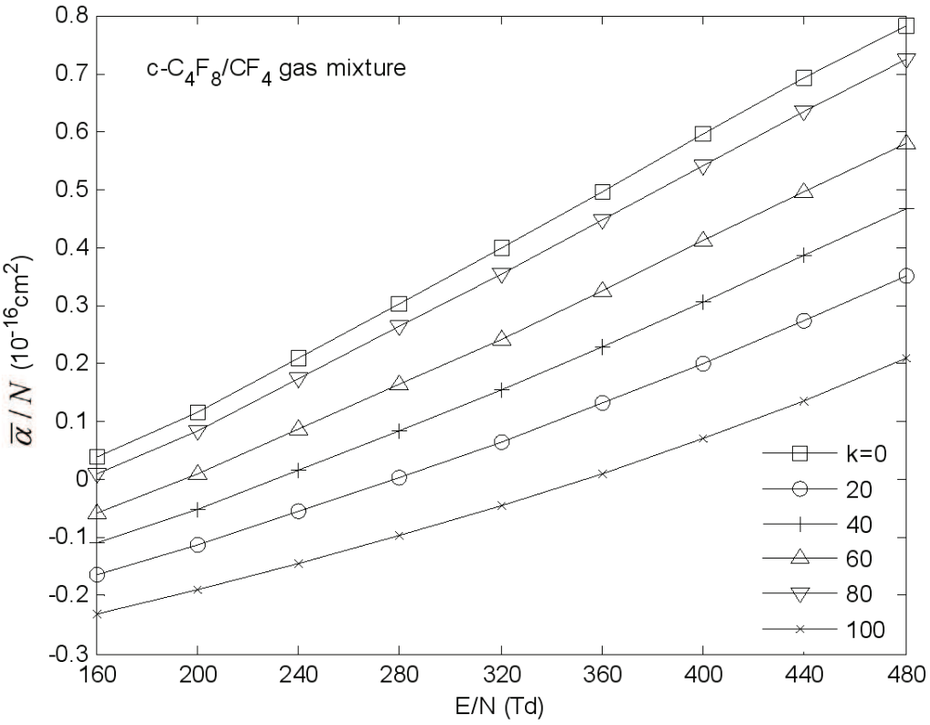

Fig. 2.18 $\overline{\alpha}/N$ of c-C_4F_8 and CF_4 gas mixtures as a function of E/N at different c-C_4F_8 gas mixture ratios k

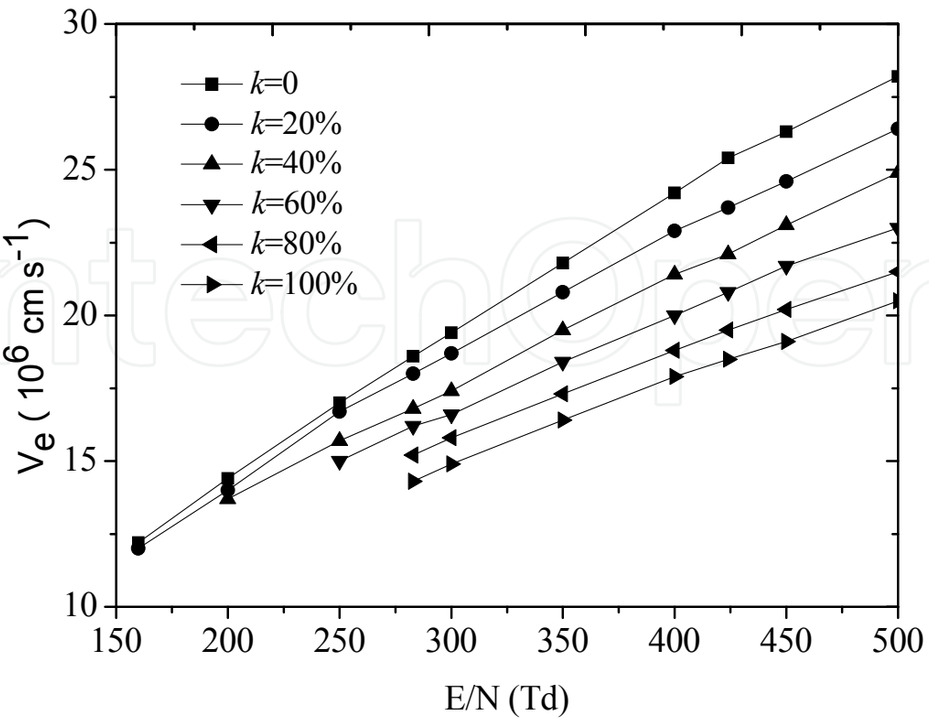

Fig. 2.19 The electron drift velocity V_e as function of E/N in c-C_4F_8/CF_4 mixtures at different c-C_4F_8 gas mixture ratios k

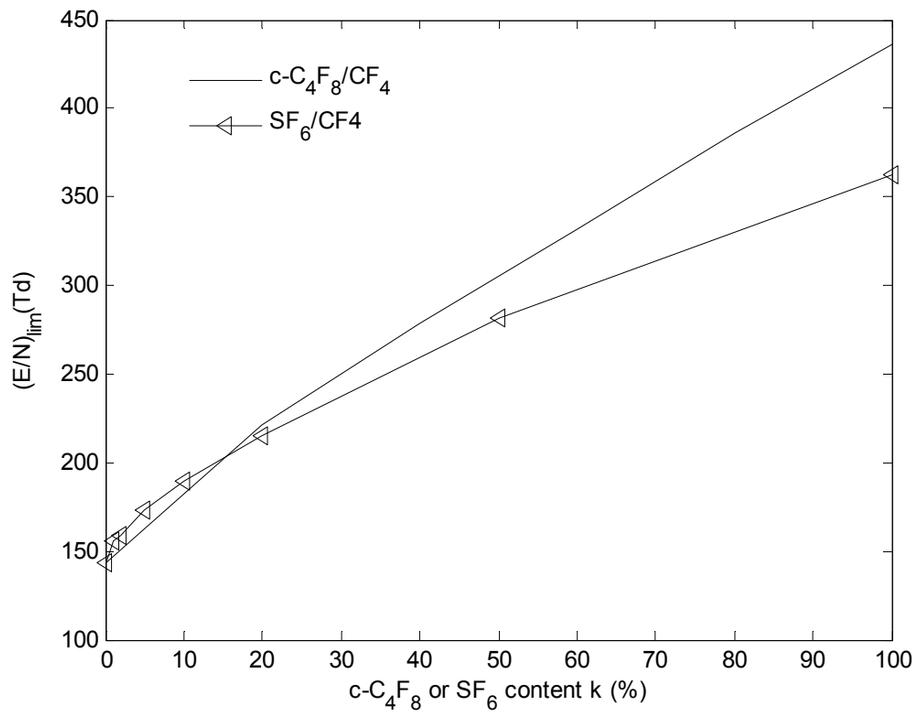

Fig. 2.20 $(E/N)_{Lim}$ of c-C_4F_8 and CF_4 gas mixtures as a function of gas content k

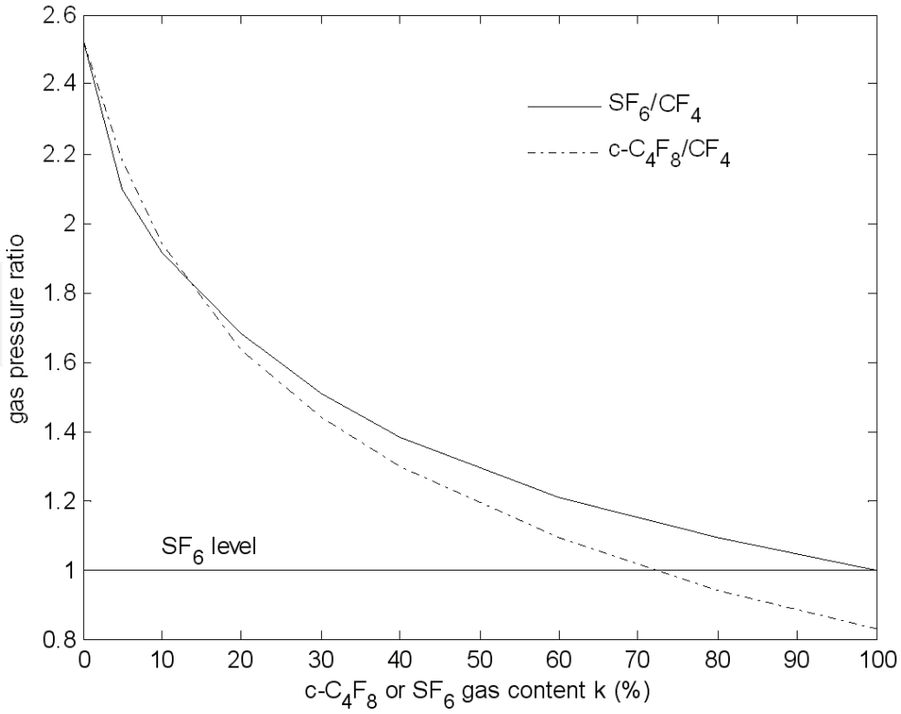

Fig. 2.21 Required gas pressure ratio of c-C_4F_8 and CF_4 gas mixtures comparable with insulation property of SF_6

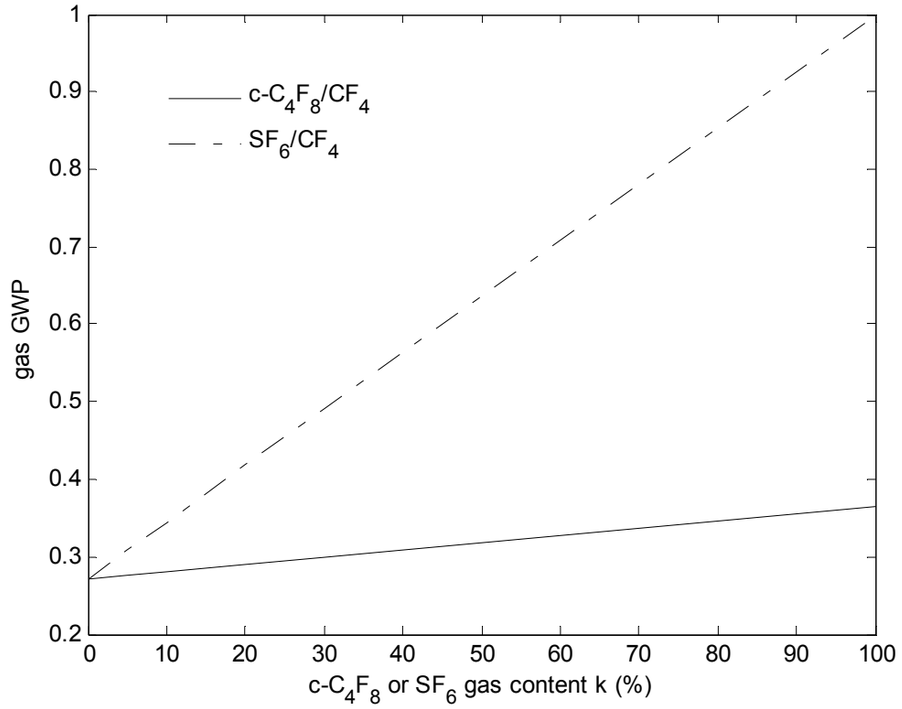

Fig. 2.22 GWP of c-C_4F_8 and CF_4 gas mixtures relative to pure SF_6

2.6.3 The avalanche discharge parameters of c-C_4F_8 and CF_4 gas mixtures

The effective ionization coefficient $\overline{\alpha}/N$ in c-C_4F_8/CF_4 changed curve with the field strength at different mixing ratio was shown in Figure 2.18, and $\overline{\alpha}/N$ decreased with c-C_4F_8 content increase, but it increased with the E/N value increases.

The electron drift velocity V_e as function of E/N in c-C_4F_8/CF_4 mixtures at different c-C_4F_8 content k was shown in Figure 2.19. With the c-C_4F_8 gas content k increased, at a fixed E/N value, the drift velocity Ve trended obvious downward. While K was at the same, Ve increased with E/N value increase. The Ve influenced greatly by CF_4 in c-C_4F_8/CF_4 gas mixtures.

The critical breakdown field strength $(E/N)_{Lim}$ of c-C_4F_8/CF_4 and corresponding SF_6/CF_4 was compared in Figure 2.20. Although the $(E/N)_{Lim}$ of SF_6/CF_4 increased rapidly at micro-mixing ratio, thus when the corresponding low electronegative gas content, SF_6/CF_4 dielectric strength slightly higher than c-C_4F_8/CF_4; but with the content K value increased, the growth rate of the former was not faster than the latter, then with K increased, the latter was more great than the former.

Figure 2.21 and Figure 2.22 respectively showed the pressure needed the corresponding insulation strength and the GWP in c-C_4F_8/CF_4 and SF_6/CF_4. To achieve the same insulation strength, the difference of the needed pressure was not great in c-C_4F_8/CF_4 and SF_6/CF_4. The greenhouse effect of c-C_4F_8/CF_4 was far less than that of SF_6/CF_4.

3. Conclusion

1. The Monte Carlo calculation model to simulate the avalanche development of the gas mixtures has set up, and the flow chart and a detailed simulation steps to simulate gas discharge have also given, to validate the feasibility of their own flight time and using null collision method, to improve the computation speed and stability of average flight distance and average flight time. On the electron moving in gas, the change of the direction of movement, energy and speed after colliding have been analyzed.
2. The improved Monte Carlo simulation method need just to deal with one collision cross section at every step, having a complex cross section for the mixed gas discharge simulation, and then the improved method can greatly improve the calculating speed. Using more mature SF_6/CO_2 to verify, the improved Monte Carlo method is feasible.
3. The gas collision cross section area used in this article have been detailed described, which cites direct the reference literature.
4. The discharge process in c-C_4F_8 and N_2, CO_2, CF_4 gas mixtures in the uniform electric field have been simulated, to find the effective ionization coefficient, electron drift velocity and the critical breakdown field strength. At the same time the greenhouse effect and the required pressure to achieve insulated strength of SF_6 have been also analyzed, and the corresponding parameters of SF_6 gas mixtures have been compared too.
5. In order to achieve the corresponding insulation strength of SF_6, the corresponding increase of pressure is similar in c-C_4F_8 gas mixtures and SF_6 gas mixture. However, the greenhouse effect of c-C_4F_8 gas mixtures is much less than that of corresponding SF_6 gas mixtures, to reduced much environmental impact.

4. Acknowledgment

This work was supported by the National Natural Science Foundation of China (No.: 50777041).

5. References

[1] Takuma T, Gas insulation and greenhouse effect, J IEE Japan 1999,119,232–235

[2] O.Yamamoto, T.Takuma, S.Hamada and Y.Yamakawa, Applying a Gas Mixture Containing c-C_4F_8 as an Insulation medium. IEEE Transactions on Dielectrics and Electrical Insulation, 2001,8(6),1075-1081.

[3] S L Lin, the null event method in computer simulation, computer physics communications,1978,15,161-163.

[4] A. SETTAOUTI and L. SETTAOUTI, simulation of electron swarm parameters in SF_6, FIZIKA A,2004, 13 (4), 121–136

[5] V D Stojanović and Z Lj Petrović, Comparison of the results of Monte Carlo simulations with experimental data for electron swarms in N_2 from moderate to very high electric field to gas density ratios (E/N), J. Phys. D: Appl. Phys,1998,31,834–846.

[6] Skullerud H R,The stochastic computer simulation of ion motion in a gas subjected to a constant electric field, BRIT.J. APPL. PHYS.1968,2 (1),1567-1568

[7] R D White, Michael A Morrison and B A Mason, On the use of classical transport analysis to determine cross-sections for low-energy e–H_2 vibrational excitation, J. Phys. B: At. Mol. Opt. Phys, 2002, 35, 605–626

[8] W Lowell Morgan, Test of a numerical optimization algorithm for obtaining cross sections for multiple collision processes from electron swarm data, J. Phys. D: Appl. Phys,1993, 26, 209-214.

[9] Blake Stacey, Relation of Electron Scattering Cross-Sections to Drift. Measurements in Noble Gases [Dissertation], MIT Undergraduate Thesis, 2005

[10] M. Suzuki et al, Momentum transfer cross section of xenon deduced from electron drift velocity data. J. Phys. D, 1992,25:50–56

[11] D K Davies, L E Kline and W E Biis, Measurements of swarm parameters and derived electron collision cross sections in methane, J Appl Phys. 1989,65(9):3311-3323.

[12] L. G. Christophorou and J. K. Olthoff, electron interaction with c-C_4F_8, J. Phys. Chem. Ref. Data, 2001,30, 449-473

[13] Masahiro Yamaji and Yoshiharu Nakamura, swarm derived electron collision cross section set for the perfluorocyclobutane molecule, J. Phys.D: Appl.Phys,2004,37, 1525-1531

[14] Kurihara. M, Petrović Z Lj and Makabe T, Transport coefficients and scattering cross-sections for plasma modelling in CF_4-Ar mixtures: a swarm analysis, J. Phys. D:Appl. Phys,2000, 33,2146-2153

[15] http://www.codiciel.fr/plateforme/plasma/bolsig/bolsig.php#get

[16] A. V. Phelps and L. C. Pitcford, Anisotropic scattering of electrons by N2 and its effect on electron transport, Phys. Rev. A,1985, 31 2932-2949

[17] Kücükarpaci H N, Lucas J, Simulation of electron swarm parameters in carbon dioxide and nitrogen for high E/N, J Phy. D: Appl Phys, 1979, 12, 2123-2137

[18] Q iu Yuchang, Kufffel E, Comparison of SF_6/N_2 and SF_6/CO_2 Gas Mixtures as Alternative to SF_6 Gas, IEEE Trans on DEI, 1999, 6 (6) : 892- 895.

[19] Xiao D M, Li X G, Xu X. Swarm parameters in SF_6 and CO_2 gas mixtures, J. Phys. D: Appl. Phys. 2001, 34: L133-L135

[20] Chan C C, Pace M and Christophorou L G, Gaseous Dielectrics I,1980, 11 ,149

[21] J de Urquijo, E Basurto and J L Herna´ndez-A´ vila, Measurement of electron drift, diffusion, and effective ionization coefficients in the SF_6–CHF_3 and SF_6–CF4 gas mixtures, J. Phys. D: Appl. Phys,2003, 36, 3132–3137

Applications of Monte Carlo Method in Science and Engineering
Edited by Prof. Shaul Mordechai

ISBN 978-953-307-691-1
Hard cover, 950 pages
Publisher InTech
Published online 28, February, 2011
Published in print edition February, 2011

In this book, Applications of Monte Carlo Method in Science and Engineering, we further expose the broad range of applications of Monte Carlo simulation in the fields of Quantum Physics, Statistical Physics, Reliability, Medical Physics, Polycrystalline Materials, Ising Model, Chemistry, Agriculture, Food Processing, X-ray Imaging, Electron Dynamics in Doped Semiconductors, Metallurgy, Remote Sensing and much more diverse topics. The book chapters included in this volume clearly reflect the current scientific importance of Monte Carlo techniques in various fields of research.

INTECH
open science | open minds

InTech Europe
University Campus STeP Ri
Slavka Krautzeka 83/A
51000 Rijeka, Croatia
Phone: +385 (51) 770 447
Fax: +385 (51) 686 166
www.intechopen.com

InTech China
Unit 405, Office Block, Hotel Equatorial Shanghai
No.65, Yan An Road (West), Shanghai, 200040, China
中国上海市延安西路65号上海国际贵都大饭店办公楼405单元
Phone: +86-21-62489820
Fax: +86-21-62489821

IntechOpen